# 18

# Applications in Complex Systems

Thomas L. White[1], T. Bond Calloway[1], Robin L. Brigmon[1],
Kimberly E. Kurtis[2] and Amal R. Jayapalan[2]
[1]*Savannah River National Laboratory*
[2]*Georgia Institute of Technology*
*United States*

## 1. Introduction

### 1.1 Introduction

Laser scanning confocal microscopy (LSCM) is widely used in biological, semiconductor, geological and other material science fields. For most non-opaque applications, interior structures can be imaged. LSCM can perform optical sectioning by acquiring images point by point and then resolve the images using a computer to provide a 3-D profile of the sample (Corle, 1996). In the past ten to fifteen years, researchers have begun to develop LSCM techniques for applications with opaque samples. LSCM technology has allowed collection of scattered, reflected or fluorescence photons to provide depth profiling of opaque samples. More importantly, advances in software for LSCMs have allowed 3-D models to be developed that provide researchers an *in-situ* view of systems that until recently have only been understood macroscopically by measuring the bulk properties of the materials. These macroscopic measurements have only allowed a conceptual understanding of the microscopic solid-solid, gas-solid and gas-solid-liquid interactions. In this chapter, we will discuss the use of LSCMs for complex opaque systems. Specific applications with complex iron-aluminum and aqueous organic slurries and cement-based composites will be discussed.

LSCM is based on the principle of eliminating stray light from "out-of-focus" flare by means of confocal apertures. Images are acquired by scanning the sample with a fixed light source, choices of laser lines, detection filters, wavelength, and by recording the light reflected from the in-focus plane with a theoretical resolution of 0.2 μm (Carter, 1999). Tomography is accomplished by recording a series of consecutive layered images in both the x-y and x-z planes. LSCM allows for the study of both organic and/or inorganic samples with minimal preparation in real time. When used to observe the outermost sample surface/subsurface areas, LSCM requires no sample preparation beyond placement on the slide. The sample is thus free from artifacts induced by drying, sectioning, or similar adulterations that are required in other analytical procedures.

### 1.2 Radioactive waste slurries applications

While the concentrated radioactive Fe/Al slurries discussed in this section are unique to the defense related nuclear industry, fundamentally processing aqueous metal slurries is done

in a variety of industries. Additionally, processing slurries containing complex aqueous organic molecules is relevant to a variety of industries. Many of the unit operations and much of the chemistry used to develop these waste processes was derived from industrial practices developed by the chemical and ceramics industries. LSCM has found applications in these industries as well. For example, LSCM has been used for examination of pore distribution (e.g. size and spatial arrangement) in ceramics for biomedical applications (Ren et al., 2005). Thus, the LSCM techniques described within this chapter are relevant to most any industry that processes opaque slurries.

The production of nuclear materials at Savannah River and Hanford Sites for the Department of Energy (DOE) resulted in the generation of radioactive waste that is currently stored in below ground storage tanks with a capacity of up to 1.3 million gallons. Each site has a goal of encapsulating the millions of gallons of radioactive waste slurry into borosilicate glass and/or grout. An involved infrastructure of facilities has been constructed or is under construction for the transportation, treatment, and immobilization of the radioactive waste slurry for long term storage.

The radioactive waste slurries are currently being immobilized in a borosilicate glass matrix using joule heated glass melters at the Savannah River Site (SRS) in the Defense Waste Processing Facility (DWPF) located near Aiken, South Carolina. A similar facility in West Valley, New York also immobilized waste generated from the reprocessing of spent nuclear fuel. Larger immobilization (vitrification) facilities are planned as part of the Hanford River Protection Project-Waste Treatment Plant (RPP-WTP) located near Richland, Washington. Highly radioactive waste is transferred to these facilities from underground tank farms. The insoluble solids content of the waste is limited by the design-basis rheological properties (e.g. the Bingham plastic yield stress and plastic viscosity) used to design the slurry transfer systems. Typically, these slurries are iron and/or aluminum hydroxides in a caustic solution.

These facilities have used or will use slurry-fed melters to safely immobilize the waste in a glass matrix. Glass forming chemicals or glass frit fabricated from glass formers is added to either the radioactive waste solutions or slurries. The resulting slurries (≈ 35 - 65 wt. % total solids) are sampled, analyzed, and then pumped to the melters. Although the DWPF process is currently operating successfully, production throughput is limited by certain bounding conditions used to design the plant (slurry rheology, glass property constraints, and in some cases, gas holdup). A simplified flow sheet of the Hanford waste treatment plant is shown in Figure 1.

The solids loading in the DWPF and future RPP-WTP melter feed slurries are limited by the rheological design bases of the mixing, sampling, and transport systems. It is desirable to increase the production rate and waste loading of the glass and therefore decrease the total quantity of waste glass produced from a total plant life cycle and cost perspective. Increasing the solids content of the melter feed would decrease the energy required to evaporate the water in the slurry, and would, therefore, increase the overall production (melt) rate of the immobilization process.

It is possible to modify the equipment used to mix, sample, and transport the waste slurry to the melter. The design and construction cost for any such modifications is very high due to the constraints (radiation and non-visible remote operation) imposed on the design and operation of radioactive waste immobilization processes. Therefore, adjustment of the

rheological properties by trace chemical addition is being explored as one option to improve the overall production rate of radioactive waste vitrification processes.

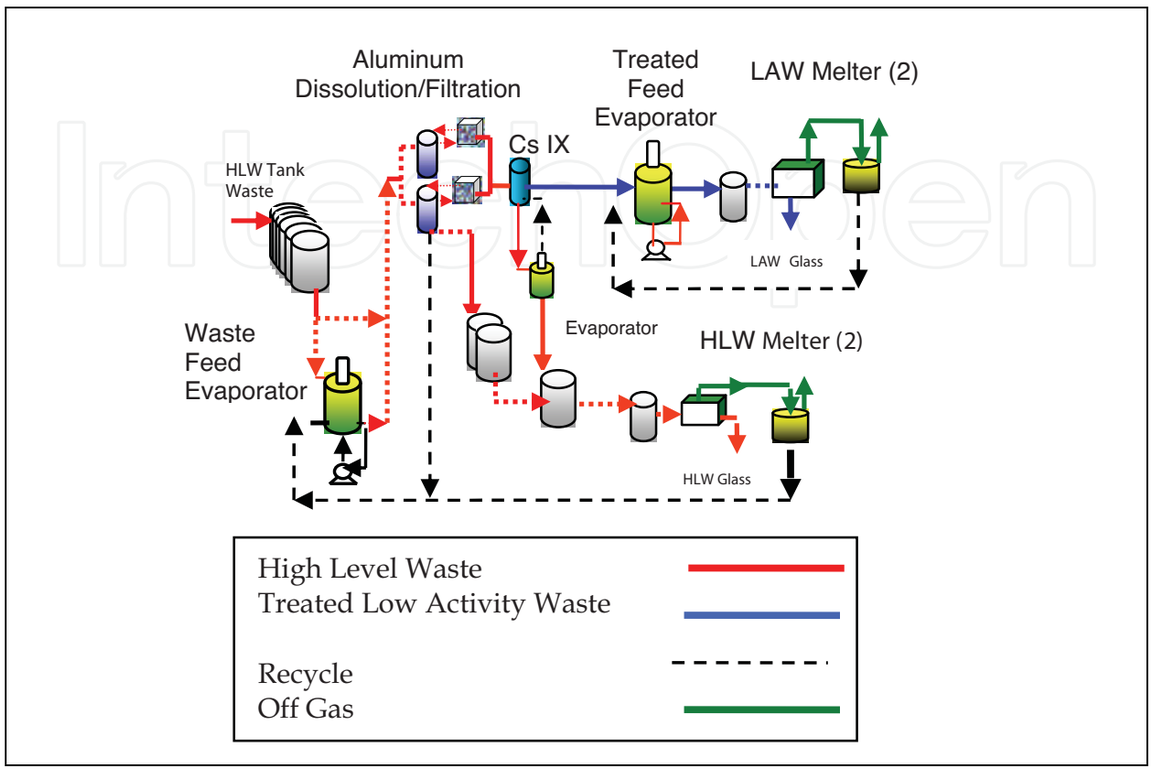


Fig. 1. Simplified flow sheet of the Hanford River Protection Project-Radioactive Waste Treatment Plant (RPP-WTP) with the dashed red/blue lines indicating unit operations involving slurries

The viscous nature of the radioactive waste slurries is also linked to operational and safety problems. Hydrogen gas produced by radiolysis can be held-up in the slurry. Understanding the hydrogen gas hold-up and release from the radioactive slurries remains a continuing research effort. Additionally, the viscous nature of these slurries causes air to be entrained in the slurry, which results in a foamy consistency, making the slurries difficult to pump. Similar problems are predicted to develop in the Hanford RPP-WTP (Kay et al., 2003, Zamecnik et al., 2003).

Nuclear waste is primarily composed of a sodium hydroxide salt supernate and transition metal sludge (See Figure 2). While the sludge is mostly inorganic oxides/hydroxides of aluminum, iron, nickel and manganese, the waste also contains sodium, carbonate, silica, oxalate, manganese, nitrite, phosphate, lead, zirconium, sulfate, potassium, nitrate as well as organic complexants and noble metals (Vijayaraghavan et al., 2006). Essentially most of the periodic table of elements is represented in nuclear waste derived from reprocessing nuclear fuel. Alumina rich sludge slurries tend to exhibit non-Newtonian rheological behavior due to floc formation increasing the viscosity and yield stress of the slurry (Ribeiro et al., 2004). At a high (≈ >45 - 50 wt. % total insoluble solids) enough solids content, the flow characteristics of the slurry can exceed the capability of the processing equipment.


Fig. 2. Non-radioactive chemical simulants of the nuclear waste containing sludge and salt supernates (Note the opaque nature of sludges that form concentrated (5 – 50%) Fe/Al slurries limiting traditional light microscopy methods)

During the DOE nuclear waste research and development effort of the 1980's, a process to remove radioactive cesium using sodium tetraphenylborate (NaTPB) to precipitate the cesium from salt supernate waste was developed. The process yielded a potassium and cesium tetraphenylborate aqueous slurry that proved to be difficult to process due to gas holdup, foaming and rheological issues (Calloway et al., 2001). Due to significant problems associated with the breakdown of tetraphenylborate to benzene, the process was eventually abandoned. Various flow sheets were explored in an effort to reduce or mitigate the effects of tetraphenylborate degradation (See Figure 3 and 4).

However, significant insight into the behavior of solid particles in slurries was developed as a part of an effort to reduce foaming in the process. These studies led to additional research into gas holdup, rheological and foaming control, and the need to better understand the behavior of particles, gases and liquids from a more fundamental microscopic level.

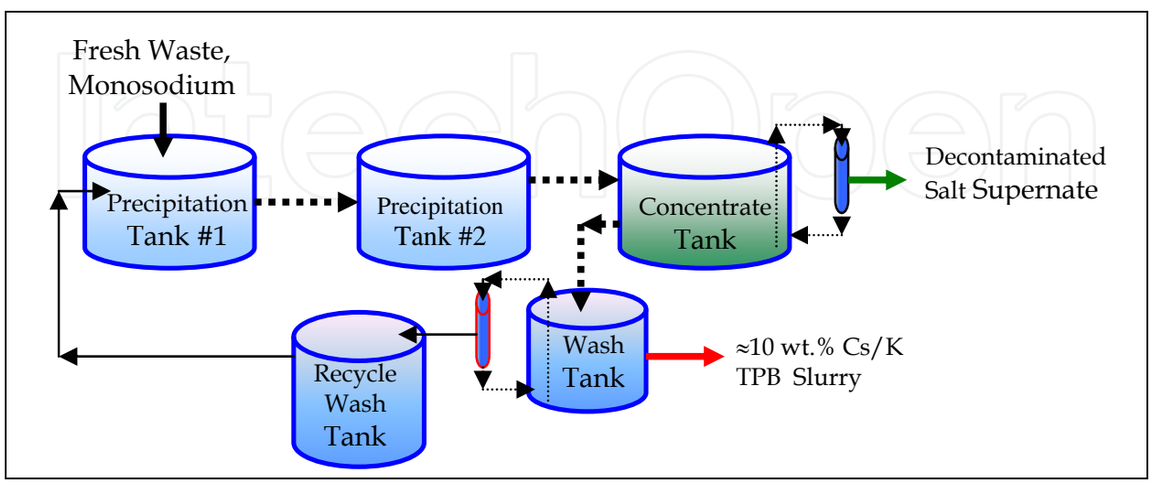


Fig. 3. Simplified flow sheet of NaTPB process to remove Cesium (Cs) from nuclear waste supernates (dashed lines indicate unit operations handling opaque slurries)

Prior to the development of LSCMs for use with opaque simulated radioactive slurries, only bulk slurry properties could be measured and the *in-situ* behavior of the particles, gases, liquids and more importantly the interface region between all three, was not well understood. These bulk measurements can also take considerable time and effort. Thus, practical development of engineering solutions to the various problems could only be accomplished empirically. Fundamental understanding of particle-gas-liquid interactions on a microscopic level has ultimately led to improved antifoam agents for nuclear waste processing facilities and should eventually help develop rheology modifiers that will allow increases in solids concentration in nuclear wastes which will increase plant throughput. Thus, further development of the LSCM slurry techniques described within this chapter should reduce the overall costs of many industrial slurry processes by furthering the understanding of the following process issues:

- Foaming/Antifoaming
- Rheology/Maximizing Solids Loadings
- Air Entrainment/Pump Cavitations

It is important for the reader to understand that LSCM is just one technique in an arsenal of analytical techniques that are available to understand complex opaque slurries. Traditional visual inspection, optical microscopy, and nuclear magnetic resonance, to more advanced neutron techniques available at national laboratories can be employed to further understand particle interactions within slurries.

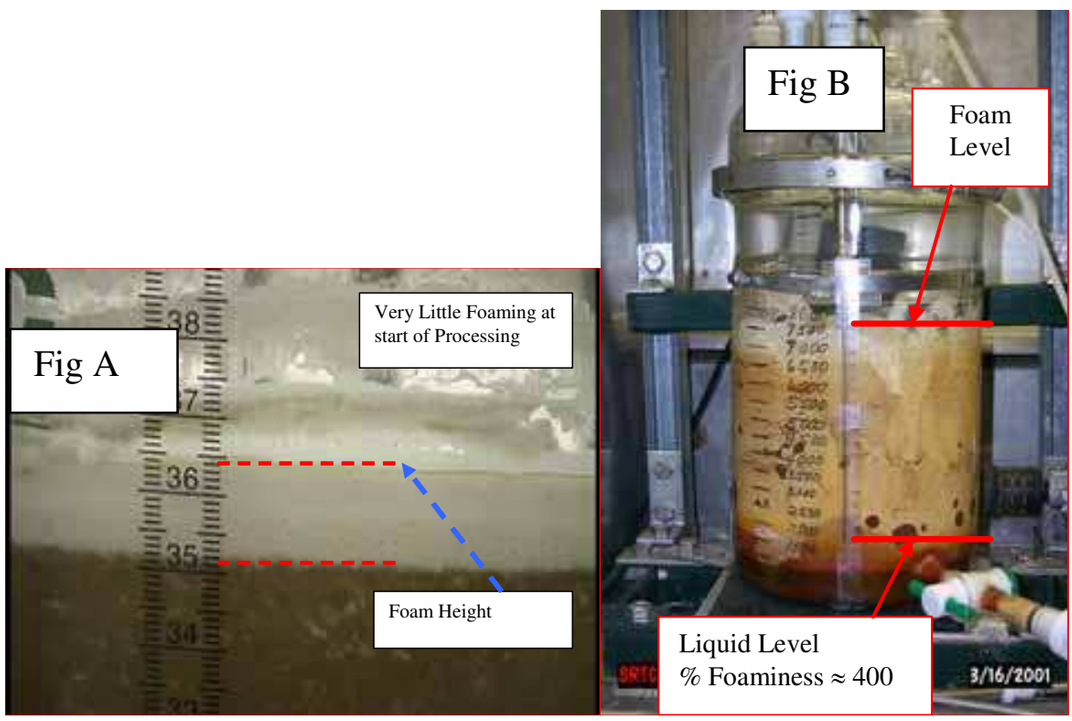


Fig. 4. Foaming and gas holdup in simulated nuclear Organic/Aqueous wastes – Fig. 4A shows foaming at the start of the process while Fig. 4B shows the dramatic change in foaming at the end of the process. The slurry is non-Newtonian and solid particles float when air is entrained in the slurry

### 1.3 Cement-based materials applications

This section will describe the application of LSCM to characterize the various interfaces that exist in cement-based materials, such as pastes, mortars, and concrete. While the use of LSCM for imaging construction materials is not as common as the use of stereomicroscopy (petrography) or scanning electron microscopy, advantages associated with LSCM over these more often applied techniques suggest that its use in this field could be increased. Using LSCM, samples can be imaged without much preparation, thus limiting the introduction of artifacts associated with drying, epoxy impregnation, or coating of samples for electron microscopy (Marusin, 1995). Because drying and coating are not required, *in situ* changes in microstructure during hydration or due to continuing deterioration can be studied using LSCM techniques (Collins et al., 2004a). Furthermore, the inherently porous surfaces, characteristic of cement-based composites as well as fracture surfaces, can be imaged by LSCM where surface asperities do not affect resolution or focus. With fracture surfaces, LSCM allows for quantification of roughness, which can be related to mechanical performance and fracture mechanics parameters (Kurtis et al., 2003; Mohr & Kurtis, 2006).

Thus, the development and use of LSCM as a characterization technique for cement-based and other construction materials has several advantages over conventional characterization methods. Here an innovative approach to the use of LSCM to examine aggregate/paste interfaces by imaging through aggregates is described (Collins et al., 2004a).

The microstructure formed at the interface between cement paste and aggregate in concrete is known to be generally weaker than both the bulk hydrated cement paste and aggregates typically used. As a result, this interface forms the "weak link" in concrete (Mehta & Monteiro, 2006). The properties of this Interfacial Transition Zone (ITZ) are thus very important and often limit the strength, stiffness and impermeability, among other properties, of concrete. The characterization of ITZ in concrete is therefore very important in understanding the physical structure and mechanical performance of cementitious composites.

A technique to study interfacial transition zones in concrete using LSCM has been developed. Here the technique is used to examine changes in concrete microstructure that occur due to a deleterious reaction called alkali-silica reaction (ASR) at the aggregate/paste interface. ASR occurs in concrete by the reaction of certain siliceous minerals found in some aggregates and alkalis which may be contributed by the cement. The reaction of such aggregates, in the presence of water, results in the formation of a potentially expansive alkali-silicate gel product. Expansion of the gel can cause cracking of concrete structures. Further details on the reaction can be found in Collins et al., 2004b.

Because the reaction essentially occurs between the aggregates and the alkaline pore solution, observations of the aggregate/paste interface are critical to understand the rate of reaction, the nature of the products formed, the mechanisms of damage, and the effects of various mitigation options. However, *in situ* imaging of the structure of the reactants present at the aggregate/paste interface, without introducing artifacts, has been challenging to achieve. This has been overcome by the use of the "through-aggregate" imaging method described herein.

## 2. Cement based materials – solid-solid system

### 2.1 Through-aggregate imaging of concrete

The through-aggregate imaging method was developed to characterize the internal aggregate/paste interfaces present in concrete. In this new technique, normal aggregate in

mortar was replaced with transparent borosilicate glass beads. In addition to obtaining images at different depths on the surface of the sample as is usually carried out with the confocal microscope, the technique allows imaging into the concrete microstructure. Thus reactions occurring inside the microstructure, especially at the aggregate/paste interface can also be studied. Three-dimensional rotational images as shown in Fig. 5 were obtained by focusing on the interfaces at various z-depths.

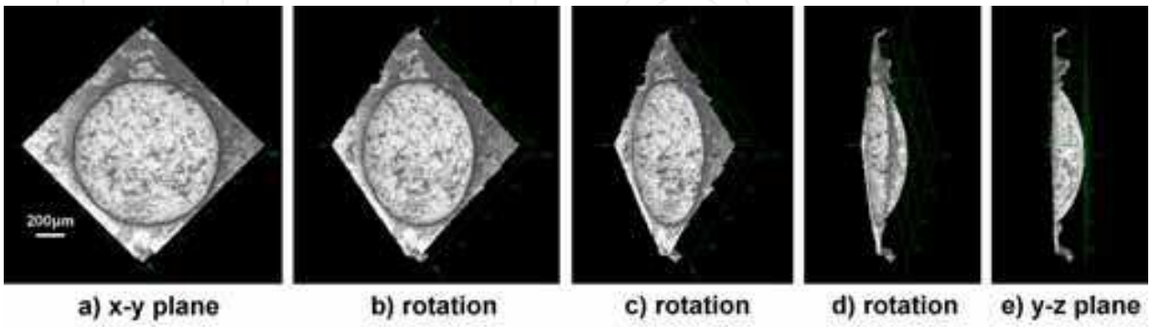


Fig. 5. Three dimensional LSCM rotational image of glass bead aggregate in mortar sample

For the study of ASR, the use of the reactive borosilicate glass beads as aggregate allows for the examination of the reaction, which is known to initiate at the aggregate/paste interface. Effective *in situ* examination of the progress of ASR was achieved using the new technique developed by imaging the same location of the sample at different stages of ASR deterioration. The samples were fixed on aluminum templates with three holes that were spaced so that the template could fit a custom-made sample stage in a unique position. Thus using the LSCM, the same locations were imaged and mapped in the x and y planes using a cross hair, indexible stage, and coordinate reader. Further details about the sample preparation and the imaging technique can be obtained from Collins et al., 2004a.

Analysis of the two-dimensional LSCM images, at various z-depths (or depths through the aggregate), shows changes in the reflected light intensity with depth and with the material being imaged (Fig. 6). At the surface of the sample, a higher light intensity was observed at the aggregate/air interface than at the cement paste/air interface, as cement absorbs more light (Fig. 6a). The intensity at the aggregate/air interface is the reflected light less the refracted light. As shown in Fig. 6b, the intensity at the aggregate/paste interface was observed to be lesser compared to the aggregate/air interface. The decrease in intensity at the aggregate/paste interface can be attributed to the multiple reflection and refraction that the light undergoes at the aggregate/air and aggregate/paste interface and also the absorption by the opaque paste at the aggregate/paste interface.

LSCM was also used to obtain two dimensional images (Fig. 7 & Fig. 8) of these mortars, similar to stereomicroscopy but with improved focus. These images can be used to track the progression of ASR damage in the sample with time. Typical indicators of damage seen in mortar or concrete undergoing ASR, such as cracking in the aggregate (Fig. 7b), increase in number of cracks and crack width (Fig. 7c), progression of cracks into the cement paste (Fig. 7c and 8b), and debonding at the aggregate/paste interface (Fig. 8a) was observed by LSCM. LSCM also allows observation of the changes occurring at the aggregate/air interface and the aggregate/paste interface with progressive ASR damage (Fig. 9). Fig. 9a shows the

reaction product that was detected in the aggregate/air interface at the surface and which was observed to extend around the aggregate/paste interface to a depth of -0.19mm, as seen in Fig. 9b . Debonding due to ASR at the aggregate/paste interface was also observed in the LSCM images; it was characterized by a complete loss of intensity of the reflected light from the aggregate/paste interface.

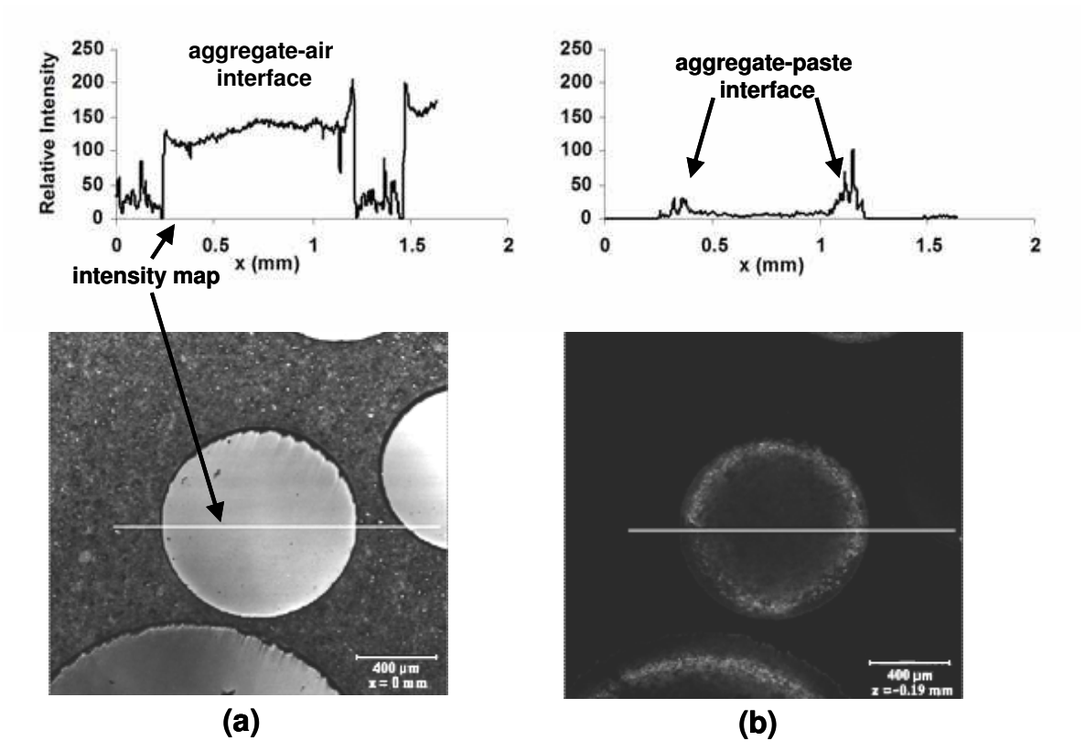


Fig. 6. LSCM images and corresponding intensity maps of the reference sample at 2 days at depths of (a) 0 and (b) -0.19mm

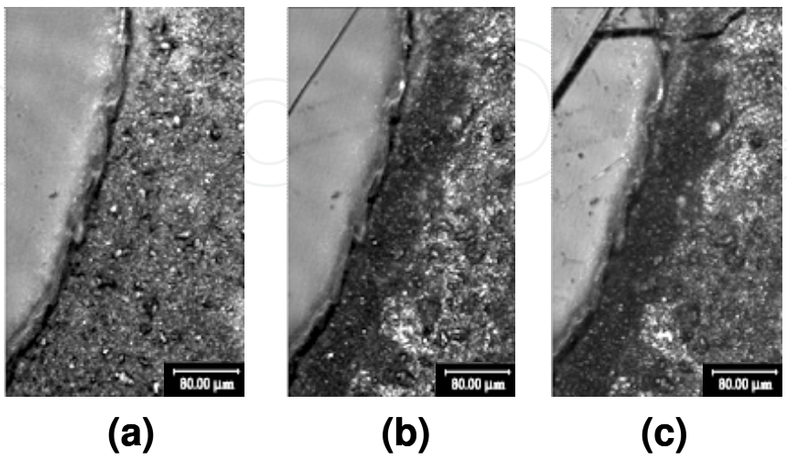


Fig. 7. LSCM images of crack formation and progression in the reference sample at (a) 2, (b) 7, and (c) 26 days

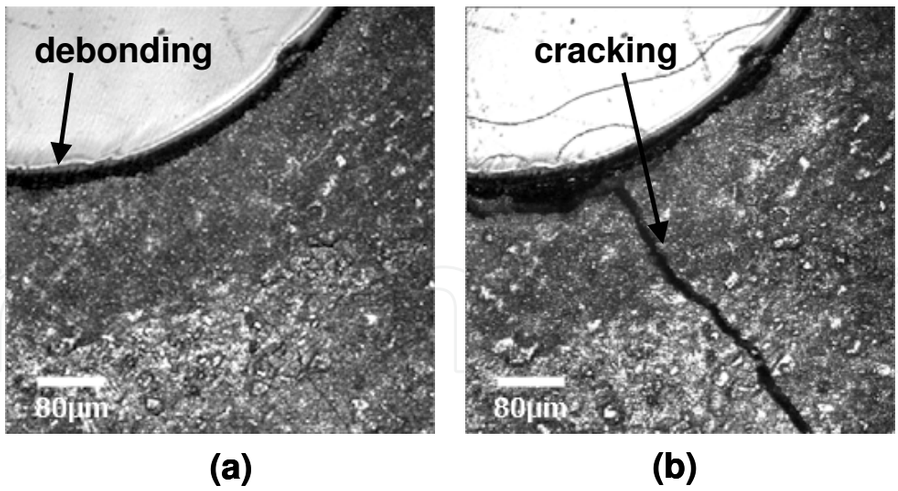


Fig. 8. LSCM images of debonding and crack progression in reference sample at (a) 7, and (b) 14 days

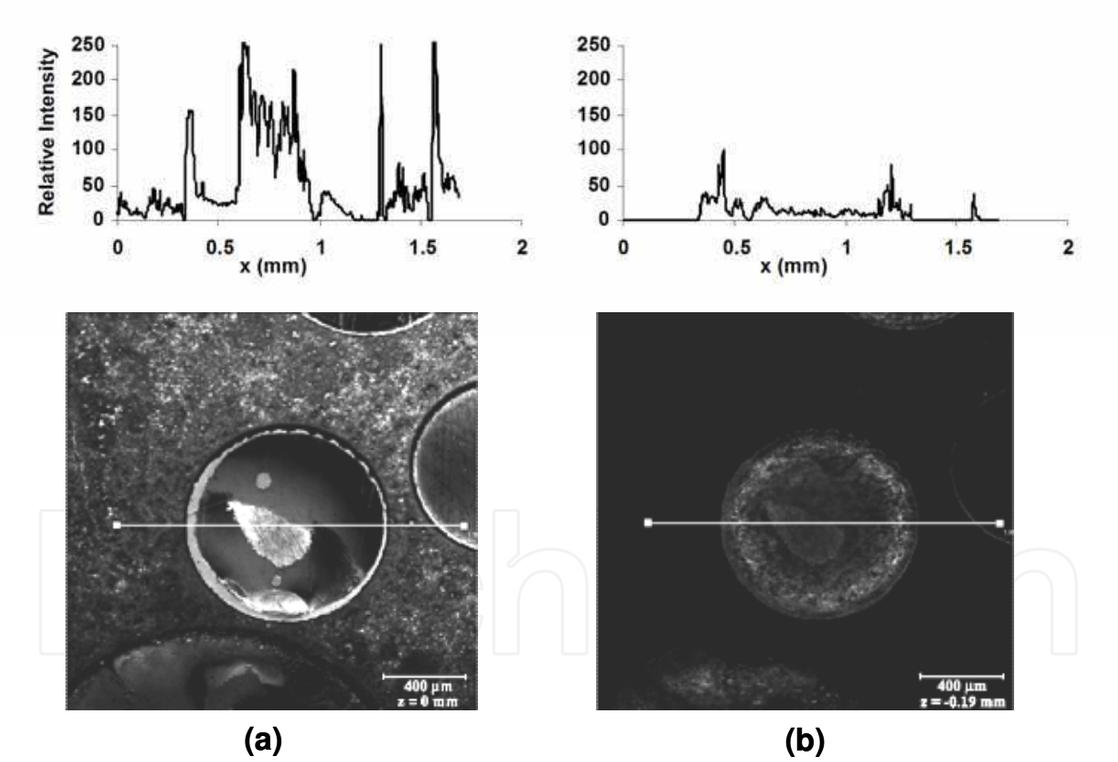


Fig. 9. LSCM images and intensity maps of the reference sample (corresponding to Fig. 6) at 67 days showing accumulation of product on the aggregate surface. The images were obtained at depths (a) 0 and (b) -0.19mm

### 2.2 Reaction products observed at aggregate/paste interface in concrete

The effect of addition of different lithium compounds (LiCl, $LiNO_3$ and LiOH) on ASR was also studied by LSCM. Lithium compounds have been shown to decrease expansion and

damage associated with ASR (Kurtis & Monteiro, 2003; Ramachandran, 1998). Here, LSCM was used to examine the changes in microstructure, especially those occurring at the aggregate/paste interface, with the addition of individual lithium compounds at specific concentrations (measured by [Li] / [Na]) to the mix water.

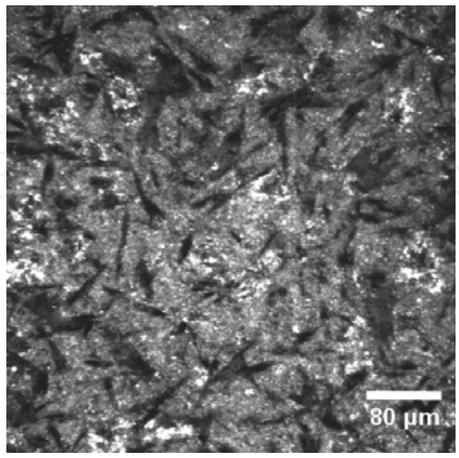


Fig. 10. LSCM image of aggregate/paste interface in sample prepared with $LiNO_3$ (Li/Na = 0.50) at 3 days

LSCM imaging showed that the samples treated with lithium chemicals (where these chemicals were added to the mix water) did not demonstrate any physical manifestations of ASR damage nor did it result in cracking due to ASR. However reaction products with a different morphology (dendritic or crystalline) were observed at the aggregate/paste interface (Fig. 10) using the through-aggregate imaging technique. It is hypothesized that these dendritic reaction products could be less expansive compared to typical ASR gel products (Collins et al., 2004a). The light intensity at the aggregate/paste interface was also reduced tremendously due to the formation of the reaction product, because of the addition of another interface in the path of travel of light.

Thus, LSCM was shown to be a very powerful technique for characterizing interfaces in concrete and in the current study alkali-silica reaction was examined using a through-aggregate imaging technique. Some of the main advantages of the technique developed which could increase the use of LSCM to characterize various cement based materials are:

- Microscopy **into** the concrete microstructure was possible using the confocal microscope;
- Compared to scanning electron microscopic imaging, this method avoids introduction of artifacts as no special sample preparation techniques such as drying and epoxy impregnation are required; and
- LSCM plane images, when compared to images obtained using a conventional microscope, are better focused even when different locations of the sample are not at the same z-level.

## 3. Radioactive waste slurries – solid-liquid system

### 3.1 LSCM applications with radioactive waste slurries

Very few researchers have applied LSCM technology to opaque concentrated slurries. (Schmid et al., 2003) and (Thill et al., 1999) applied LSCM technology to activated waste

water sludges to determine volumes, heterogeneity factors, compositions of bacterial population and aggregate size. (Kay et al., 2003) developed the first laser confocal images of concentrated (>10 wt. %, See Fig. 2) Fe/Al simulated radioactive sludges. The motivation for this effort was to begin to understand how slurry yield stress and viscosity could be improved and to understand the actual internal slurry structure.

The three dimensional representation shown in Figure 11 represents the true power of LSCM for opaque slurry applications (Kay et al., 2003). This technique allows the slurry to be analyzed in an *in-situ* condition. The microscope has the ability to make both two-dimensional pictures and three-dimensional representations of a sample. In the case of Figure 11, three-dimensional representations were made by scanning two-dimensional images at 1-micron increments. Image analysis software provided by Carl Zeiss, Inc. was used to stack the images together in a two dimensional image that provides a color gradient corresponding to the depth of the sample. These three-dimensional representations were used to understand the actual physical structure of the slurries. The slides with simulated waste (wet) samples were mounted using 2 drops of the material on a glass slide covered with a cover slip. A drop of oil was added to the top of the cover slip to view through oil immersion at 1300X. Slides were then examined and select images saved with a Laser Scanning Confocal Microscope (Model 310 Carl Zeiss, Inc., Thornwood, NY).

Figure 11 shows a three-dimensional representation of the RPP-WTP AZ102 slurry (Control, similar to opaque sludge shown in Fig. 2) using a LSCM. The scale in the upper left-hand corner shows the depth of the image. The scale in the lower portion of the image shows the horizontal scale. The red, green, and blue colors correspond to a depth of 0, 7.5, and 15 microns in the slurry sample. The AZ102 slurry particles shown in Figure 11 appear to be flocculated into larger (> 5 micron) size flocs. These flocs are suspended by smaller particles. Figure 11 appears to indicate the slurry is a flocculated, touching network of particles (Kay, 2003, Pugh, 1994). Figure 11 represents the first 2D three dimensional *in-situ* model of simulated radioactive high level waste slurry. Figure 12 is one of the two dimensional images that was used to develop the three dimensional model (one or the other 2D vs 3D) shown in Figure 11.

### 3.2 Dispersant use with slurries

A number of industries handle concentrated slurries such as ceramic (Chou & Senna, 1987), paint (Fujitani, 1996; Auschra et al., 2002), ink (Spinelli, 1998) and coal (Baxter & Habib, 1992). Transportation and processing of these slurries is often necessary highlighting the need to understand and control the solid-liquid mixture's response to flow. The rheological properties of the mixture are influenced by the solids content, particle size (Dabak & Yucel, 1987) and shape, particle interaction (Frith et al., 1987) and the solvent characteristics (Russel, 1987). In water, solids such as alumina can interact through interparticle forces to form flocs leading to non-Newtonian rheological behavior. These flocs immobilize some liquid essentially increasing the effective solid volume and thus the viscosity of the solid-liquid mixture increases (Garrido & Aglietti, 2001). Dispersants are added to improve the flow and handling characteristics of the slurry. Polymeric dispersants, such as polyacrylates, are designed with a hydrophilic segment and a hydrophobic segment. Solids are encapsulated by the dispersant with the hydrophobic portion absorbed onto the particles and the hydrophilic portion extending into the water. Deflocculation occurs with both steric

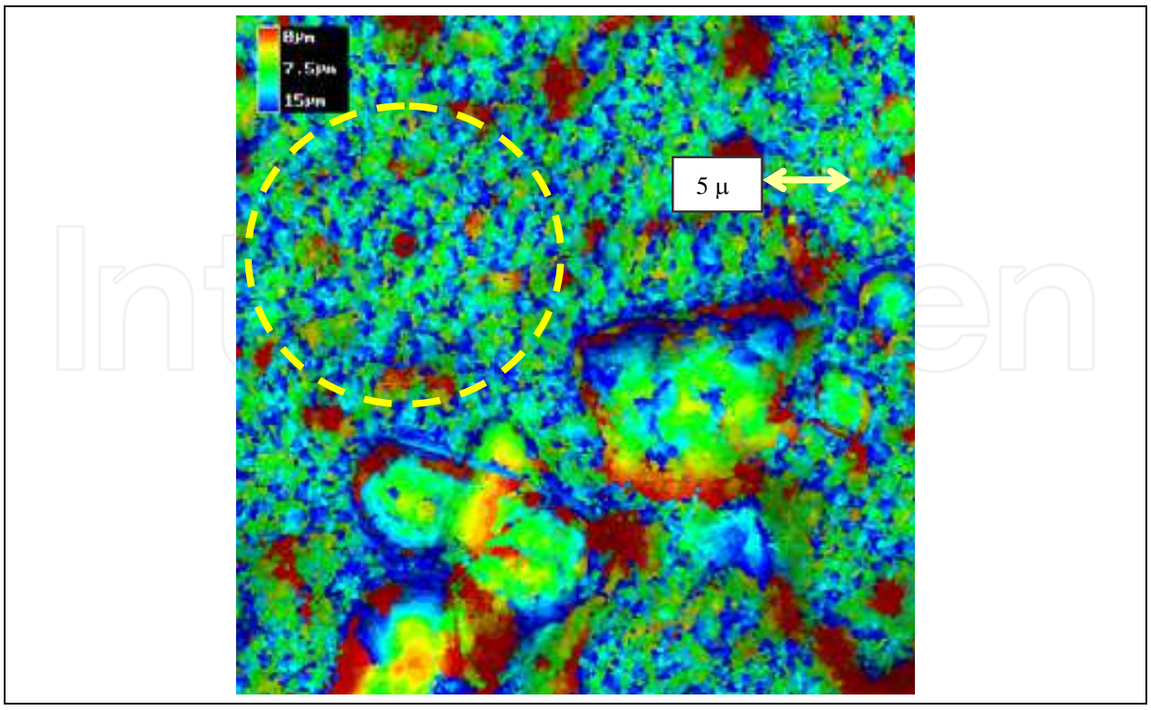


Fig. 11. Three dimensional representation of simulated AZ102 Hanford slurry with the area within the yellow dashed circle showing the most representative sample of the slurry

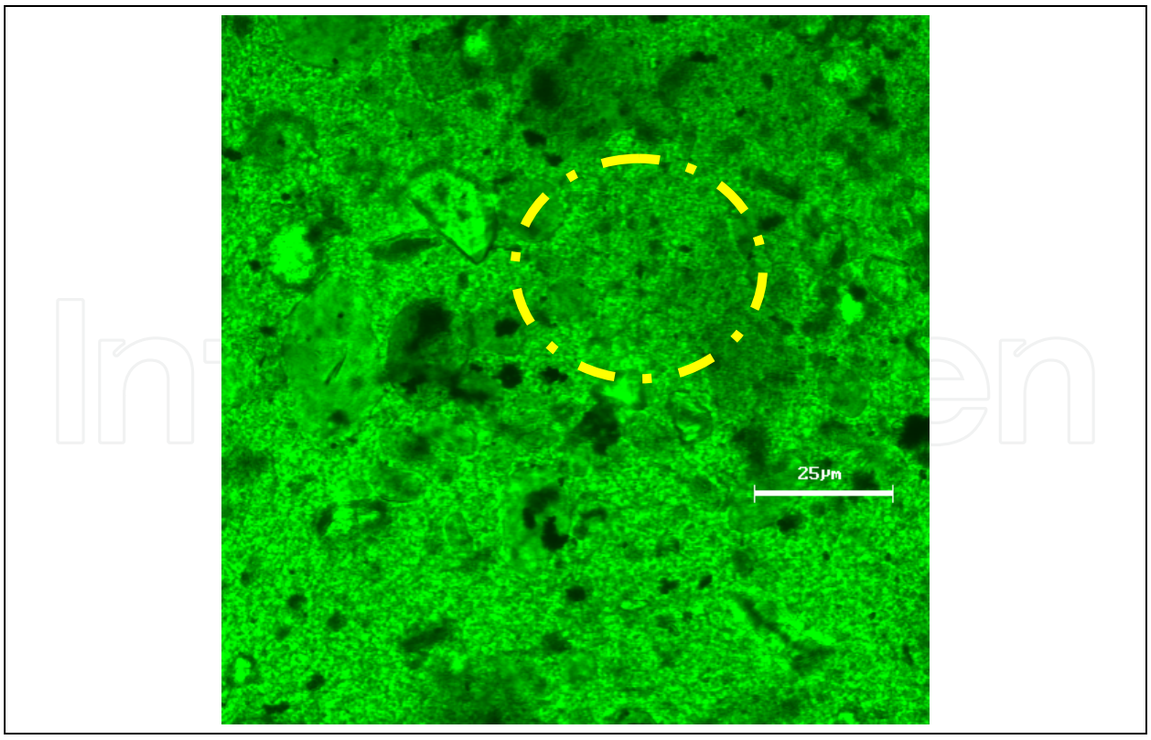


Fig. 12. Two-Dimensional view of simulated radioactive Hanford slurry AZ-102 with particles less than 25 micron (µm) in size shown in the dashed circle

and ionic stabilization of the particle. Treatment of solid-liquid mixtures with the appropriate dispersant can lead to near Newtonian rheological behavior and improved liquid flow properties especially at higher solids content (Ribeiro et al., 2004).
Other applications and references using LSCM technology to explore the effects of surfactants on various systems are discussed in the solid-liquid-gas systems section of this chapter.

### 3.3 The rheology of simulated radioactive waste with dispersant

The use of dispersants has been examined on simulated radioactive waste to improve flow properties of slurries (White et al., 2008, Kay et al., 2003). Plate-to-plate rheological measurements of the 20 wt% simulated waste slurries with and without polymeric dispersant showed at least 30% decrease in the yield stress for the dispersant containing samples as shown in Table 1. The baseline simulated waste slurry yielded a rheology curve that is typical for Bingham fluids (Figure 13) with a high initial yield stress (Dean et al., 2007). Equation 1 describes the two parameter rheology model that is used extensively in the drilling fluids industry to describe the flow characteristics of many different types of muds. These fluids require a certain amount of stress to initiate flow at the yield point (YP) and do not have a constant viscosity. The plastic viscosity (PV) is the slope of the shear stress ($\tau$)/shear rate ($\gamma$) line above the yield point (YP). These results are consistent with what has been observed with Al-rich sludges in the ceramic industry as is the drop in yield stress when dispersant is added (Ribeiro et al., 2004). As more dispersant is added, the slurry becomes less pseudoplastic in character and trends toward Newtonian behaviour.

$$\tau = YP + PV(\gamma) \tag{1}$$

Where
$\tau$ = shear stress
YP = yield point
PV = plastic viscosity
$\gamma$ = shear rate

| | Yield Stress, Pa | | | | |
|---|---|---|---|---|---|
| # | Description | Up Ave. | % Diff. | Down Ave. | % Diff. |
| 1 | Baseline | 14.0 | NA | 13.2 | NA |
| 2 | 3000 ppm Dolapix CE64 | 7.79 | 44.2 | 5.97 | 54.8 |
| 3 | 3000 ppm Disperse-Ayd W28 | 8.83 | 36.7 | 7.65 | 42.1 |
| 4 | 3000 ppm Cyanamer P35 | 9.5 | 31.9 | 8.78 | 33.6 |

Table 1. Rheology data in duplicate for simulated radioactive waste slurries

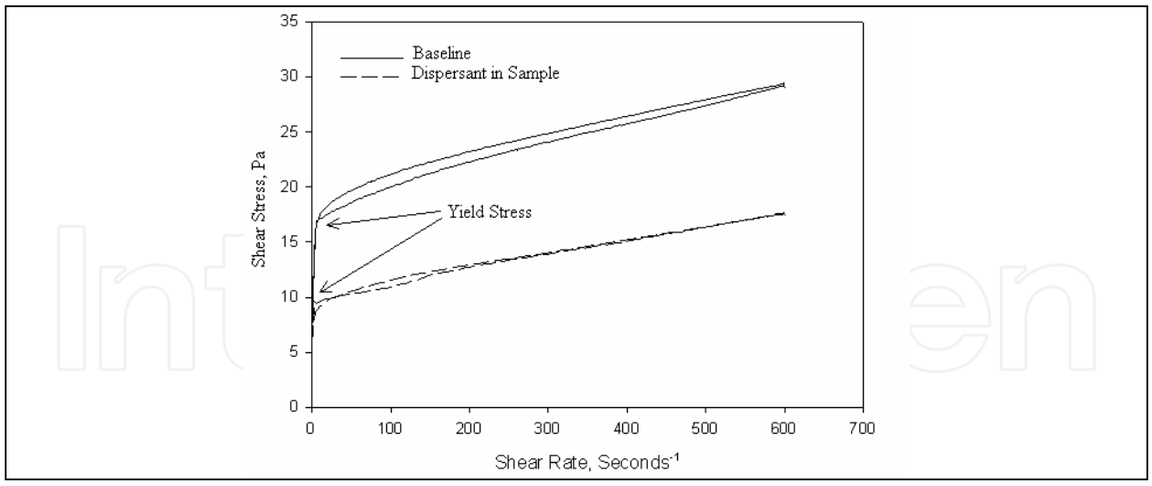


Fig. 13. Effect of dispersant on simulated radioactive waste slurries (Note the sample with dispersant has a lower yield stress moving to curve to more Newtonian behaviour)

### 3.4 Examination of simulated radioactive waste with dispersant

To better understand the effect of the dispersants, a direct method rather than a bulk method such as rheology was employed. LSCM offered a way of directly observing the solid-liquid mixtures with depth profiling on a micrometer scale. This capability allows the researcher to observe changes in the material due to dispersant addition and assess if particle stability is occurring. For the simulated radioactive waste work (White et al., 2008), samples were prepared on a Sedgewick Rafter slide that contains a chamber (50 mm l x 20 mm w x 1 mm d) suited for containing a drop of slurry. A glass cover was carefully placed over the liquid taking care to avoid bubble formation. This sample mounting method allows for viewing of the slurry as an undisturbed drop. The solid-liquid mixture (20%wt, 1-5 μm particles) was viewed under low (100x) magnification as shown in Figure 14 A & B. Large aggregates, many near 50 μm, can be observed in Figure 14 A that are not present in Fig. 14 B. The Z-contrast detailed the unique three-dimensional structural information as shown in Figure 14 C & D and was formed by repeatedly scanning at designated depths of 40 images at 10 μm intervals. The topography shows large aggregates present in image C without dispersant and not in image D where particles have been stabilized with dispersant. These images successfully portray the deflocculation of the simulated waste expected from the rheology results on a μm scale. It would be useful to continue developing methods such as specific dyes that highlight the dispersant for contrast and higher magnification to see below the μm scale to the particle edge.

## 4. Radioactive waste slurries – solid-liquid-gas systems

A majority of foams are comprised of two phases, typically a gas and liquid-either aqueous or organic-containing surfactants. However, foams containing three phases (i.e., gas, liquid and solid particles) are also encountered in industry; for example, in the processing of solid wastes, food, chemical, and agricultural products. Radioactive waste presents some of the most complex foam-forming systems (Vijayaraghavan et al., 2006; Calloway et al., 2001). Wasan et al. (2004) have identified at least two kinds of particles in such three phase gas-solid-liquid systems: hydrophilic (i.e., water-wet) and amphiphilic or Janus (i.e., biphilic, partially wetted by water). The Janus particles are formed due to the non-uniform

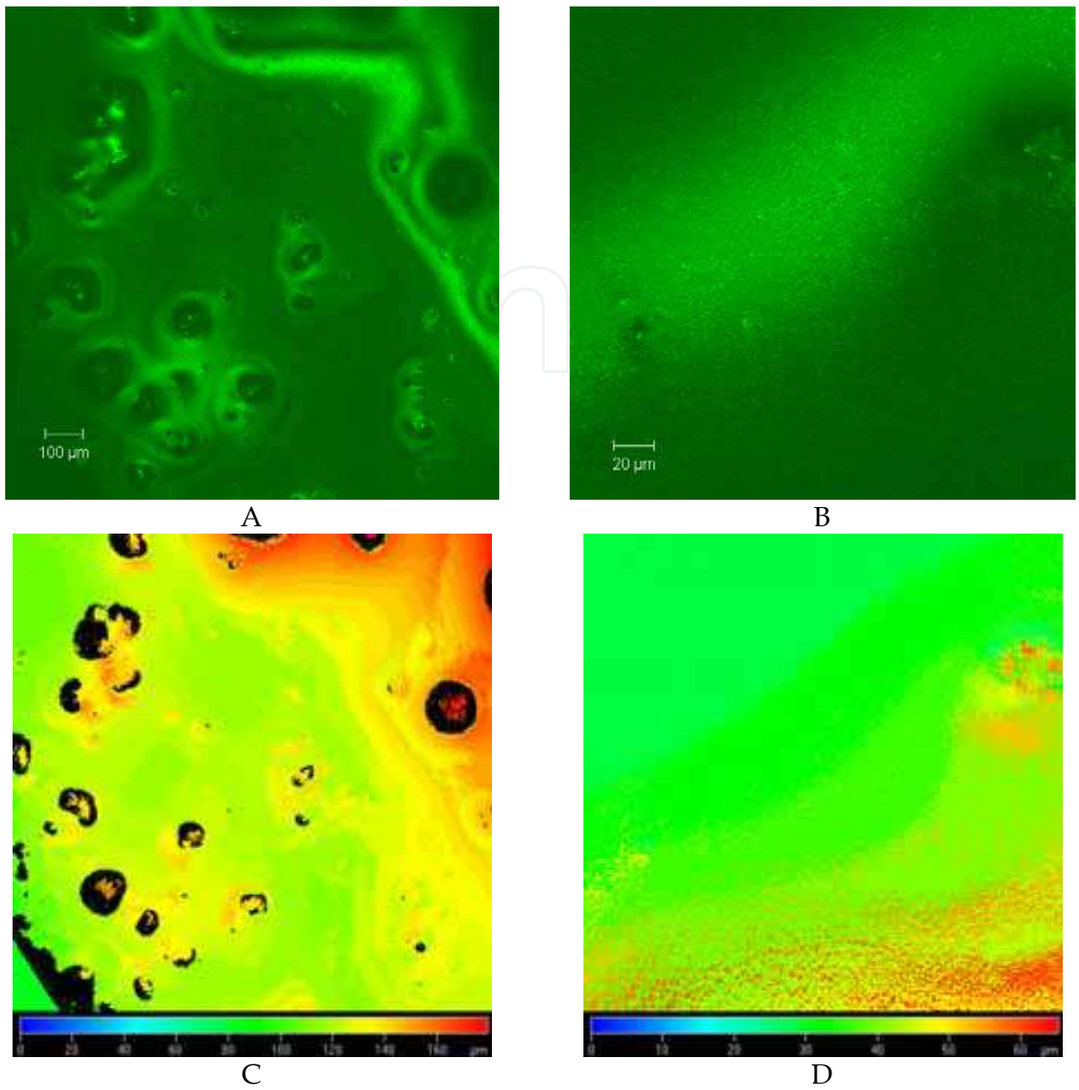


Fig. 14. LSCM images of baseline-simulated radioactive waste slurry (A & C) and simulated radioactive waste slurry with dispersant (B & D) (Note the loss in large aggregates)

surface energy of crystalline materials present in the wastes (Bindal et al., 2001, Binsk & Fletcher 2001). Solids which are not readily wetted with water (i.e., Janus), tend to migrate to a liquid-vapor/gas interface. At the interface, the solids essentially block the liquid in the foam from draining and therefore increase the stability and duration of the foam.

Various researchers have explored the use of LSCM to investigate the nature of the solid-liquid-gas interface in foams (Liu et al., 2009; Zhang et al., 2008; Fujii et al., 2006; Reed et al., 1997; Lau & Dickinson, 2005; Dong et al., 2010). Zhang and subsequently Liu investigated aqueous foam stabilized with Laponite particles modified by a surfactant. Laponite forms a nearly clear fluid in aqueous systems and makes an ideal model system for exploring various effects of surfactants and solids concentration on slurries. Typically, researchers investigating Laponite systems use Rhodamine B, which is negatively charged in a basic solution and has a maximum excitation wavelength at 543 nm. The modified Laponite particles were in effect "labeled" by the fluorescently active Rhodamine B. Excess

Rhodamine B was washed from the particle dispersions with deionized water. The LSCM was then used to image the particles "labeled" with Rhodamine B. In the Laponite application, the LSCM was used to image how the partially hydrophobic or "Janus" particles attached to the gas bubble surface. Fujii examined latex-stabilized aqueous foams by LSCM in which the laser was operated at wavelengths of 351 nm for excitation of the pyrene groups in the polystyrene matrix. Reed and co-workers developed an actual three-dimensional image of the foam lamella in which the 3D effect can be viewed with the appropriate red/green glasses. The liquid portion of the solution was ethanol and fluorescein allowing viewing of the liquid fraction of the foam, thus revealing the complex three dimensional structures. Lau used the LSCM to monitor a long sequence of foam images at closely spaced intervals to study the dynamic nature of foams over time.
Researchers at the Savannah River National Laboratory developed a LSCM method to capture a complete picture of the Janus particles at the liquid-vapor/gas interface. Figure 15 shows a two-dimensional image of potassium tetraphenylborate particles (e.g., Janus particles) attached to a foam bubble in the slurry. In this application, excess tetraphenyl borate ions in solution and possibly benzene and other trace organic breakdown products are excited by the laser. In this case, the "Janus" particles are surrounding the air bubble.

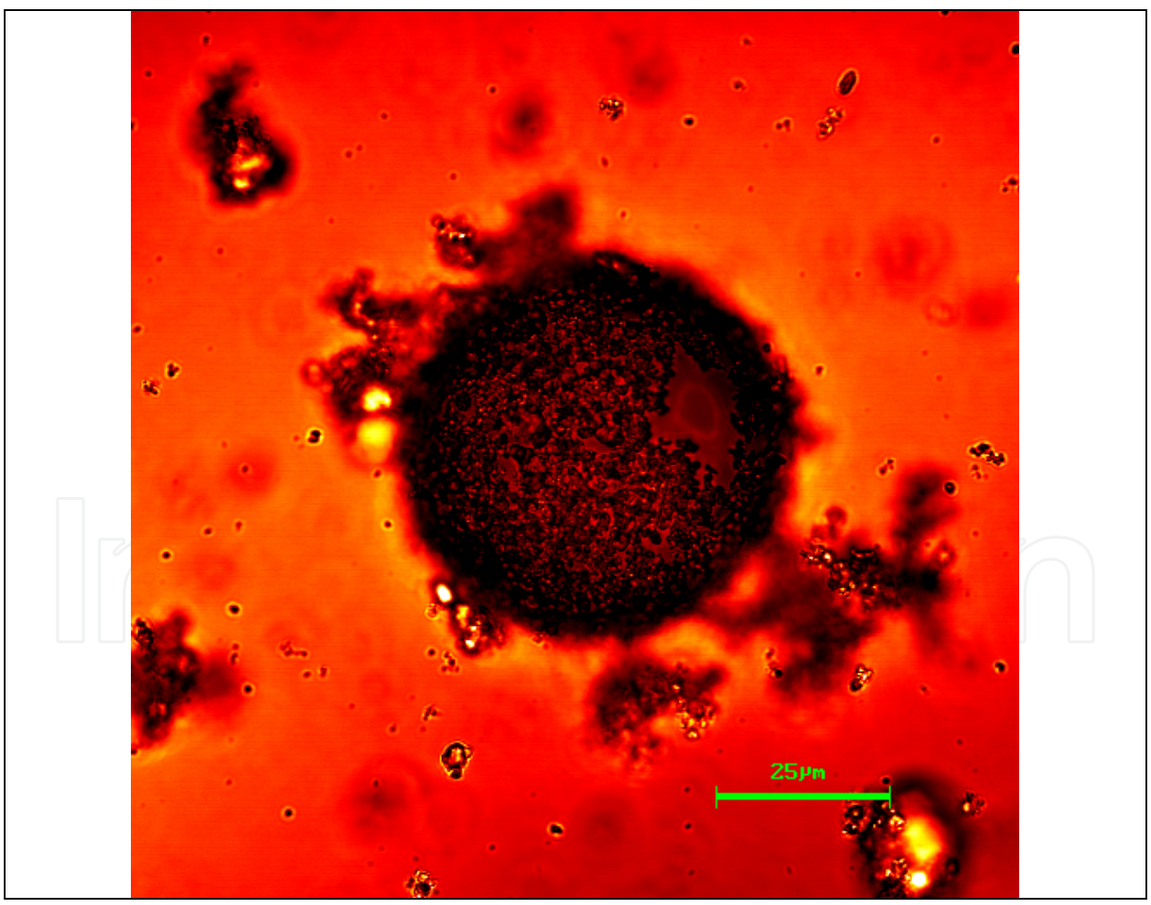


Fig. 15. LSCM image of simulated nuclear waste foams. Janus particles are clearly attached to the liquid-gas interface. Fundamental understanding of these systems has been used to develop new antifoams. Note size of bubble is greater than 25 um in diameter

The slides with simulated wet waste samples were mounted using 2 drops of the material on a glass slide covered with a cover slip. A drop of oil was added to the top of the cover slip to view through oil immersion at 1300X. Slides were then examined and select images saved with a Laser Scanning Confocal Microscope (Model 310 Carl Zeiss, Inc., Thornwood, NY). The slurry was not treated with antifoam agent (surfactant).
Further slides (See Figure 16) of the same NaTPB slurry sample reveal a complex network of foam within the slurry which also explains why the solid particles actually float to the surface of the solution.

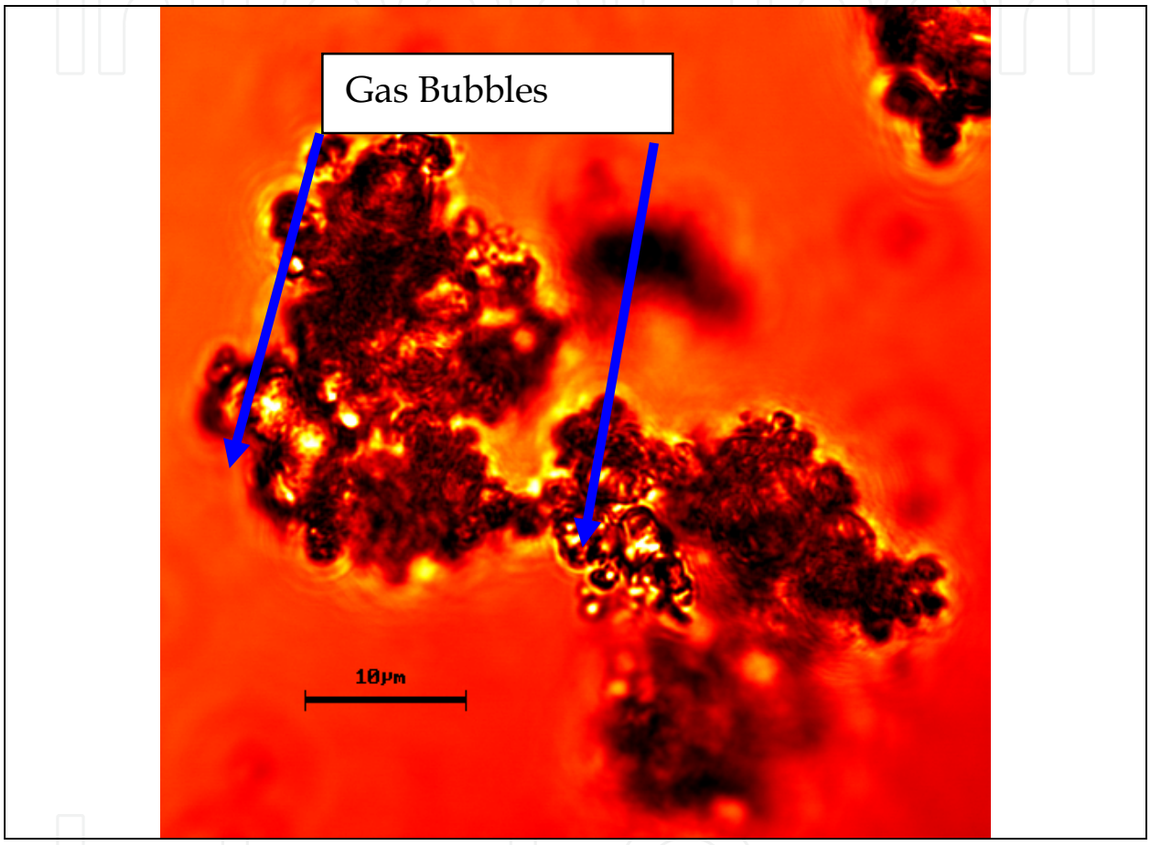


Fig. 16. View of NaTPB foam (Note the entrained bubbles within the solid particles- Entrained gas allows the solid particles to float to the surface)

## 5. Conclusion

This work demonstrates that LSCM is a useful tool for direct imaging of both complex solids and slurries. The integrity of cementitious materials may be examined by imaging the microstructure for cracking and debonding (Fig. 7 & Fig. 8) and various interfaces for the formation of reaction products (Fig. 9 & Fig. 10). Small scale changes such as gas bubble formation in slurries (Fig. 16), a critical factor in the process, may be highlighted. Particle stabilization with dispersant (Fig. 14) can be imaged and studied. Once a set of optimum parameters has been found for a given material, they can be used and quickly adjusted for rapid imaging. Considerable effort is needed to set up operating conditions such as the optimum laser, filter, and wavelength. In addition, sample preparation needs to be

considered. Several mounting formats were tested before the Sedgewick-Rafter slides were found to preserve the integrity of the slurry sample during imaging by eliminating drying or introducing other artifacts.

Future work should focus on improved image contrast using stains and flurochromes specific to the sample to highlight regions. Further, image improvement gains can be achieved by applying improved image processing software. Finally, novel methods of sample preparation, if required, prior to imaging are critical and should continue to be refined.

## 6. Acknowledgement

The authors Kurtis and Jayapalan would like to thank Courtney Collins for the contributions to this research project. They also acknowledge the support to this project by the U.S. National Science Foundation POWRE Award CMS-0074874 and Grant No. CMMI-0825373. Any opinions, findings, and conclusions or recommendations expressed in this material are those of the authors and do not necessarily reflect the views of the National Science Foundation.

## 7. References

Aguilera, J. & Stanley, D. (1999). Examining food microstructure, In*: Microstructural Principles of Food Processing and Engineering*, (2nd), (19 - 22), Aspen Publishers, 0-8342-1256-0, Gaithersburg, Maryland

Aushra, C.; Eshstein, E. ; Mühlebach, A.; Zink, M. & Rime, F. (2002). Design of new pigment dispersants by controlled radial polymerization. *Progress in Organic Coatings*, 45, 2-3, (October 2002) (83-93), 0300-9440

Baxter, L. & Habib, Z. (1992). The effect of surfactants on disaggregation of coal-water slurry particles during combustion. *Combustion and Flame*, 90, 2, (August 1992) (199-209), 0010-2180

Bearsley, S.; Forbes, A. & Haverkamp, R. (2004). Direct observation of the asphaltene structure in paving-grade bitumen using confocal laser-scanning microscopy, *Journal of Microscopy*, 215, 2 (August 2004), (149-155), 0022-2720

Bindal, S.; Nikolov, A.; Wasan, D.; Lambert, D. & Koopman, D. (2001). Foaming in simulated radioactive waste, *Environmental Science & Technology*, 35, 19, (October 2001) (3941-3947), 0013-936X

Binsk, B. & Fletcher, P. (2001). Particles adsorbed at oil-water interface: a theoretical comparison between spheres of uniform wettability and "Janus" particles, *Langmuir*, 17, 16, (August 2001) (4708 – 4710), 0743-7463

Calloway, T.; Baich, M. & Lambert, D. (2001). Fate of IITB52 Antifoam Across the Small Tank Tetraphenylborate Process, WSRC-TR-2001-00102, http://www.osti.gov/bridge/product.biblio.jsp?query_id=0&page=0&osti_id=783018

Carter, D. (1999). Practical considerations for collecting confocal images, In: *Methods in Molecular Biology*, *Confocal Microscopy Methods and Protocols*, Stephen W. Paddock, (122), (35-57), Humama Press, 0-89603-526-3, Totowa, New Jersey

Chou, C. & Senna, M. (1987). Correlation between rheological behavior of aqueous suspensions of $Al_2O_3$ and properties of cast bodies: effects of dispersants and ultrafine powders. *American Ceramic Society Bulletin*, 66, 7, (Jule 1987) (1129-1133), 0002-7812

Chou, K. (1989). Effect of dispersants on the rheological properties and slip casting of concentrated alumina slurry. *J Am. Ceram. Soc.*, 72, 6, (September 1989) (1622-27), 0002-7820

Collins, C.; Ideker, J. & Kurtis, K. (2004a). Laser scanning confocal microscopy for *in situ* monitoring of alkali-silica reaction. *Journal of Microscopy-Oxford*, 213, (February 2004) (149-157), 0022-2720

Collins, C.; Ideker, J.; Willis, G. & Kurtis, K. (2004b). Examination of the effects of LiOH, LiCl, and $LiNO_3$ on alkali-silica reaction. *Cement and Concrete Research*, 34, 8, (August 2004) (1403-1415), 0008-8846

Corle, R., Kino, S. (1996). *Confocal Scanning Optical Microscopy and Related Imaging Systems*. Academic Press, 0-12-408750-7, San Diego, CA

Dabak, T. & Yucel, O. (1987). Modeling of the Concentration and Particle Size Distribution Effects on the Rheology of Highly Concentrated Suspensions. *Powder Technology*, 52, (October 1987) (193-206), 0032-5910

Dean, E.; Glowinski, R. & Guidoboni, G. (2007). On the Numerical Simulation of Bingham visco-plastic flow: Old and New Results. *J Non-Newtonian Fluid Mech.*, 142, (March 2007) (36-62), 0377-0257

Dong, X.; Xu, J.; Cao, C.; Sun, D. & Jiang, X. (2010). Aqueous foam stabilized by hydrophobically modified silica particles and liquid paraffin droplets, *Colloids and Surfaces A: Physicochem. Eng. Aspects*, 353, 2-3 (January 2010) (181-188), 0927-7757

Frith, W.; Mewis, J. & Strivens, T. (1987). Rheology of concentrated suspensions: experimental investigations, *Powder Technology*, 51, (June 1987) (27-34), 0032-5910

Fujii, S.; Iddon, P.; Ryan, A. & Armes, S. (2006). Aqueous particulate foams stabilized solely with polymer latex particles, *Langmuir*, 22, 18, (August 2006) (7512-7520), 0743-7463

Fujitani, T. (1996). Stability of pigment and resin dispersions in waterborne paint. *Progress in Organic Coatings*, 29, 1-4, (September-December 1996) (97-105), 0300-9440

Garrido, B. & Aglietti, F. (2001). Effect of rheological properties of zircon-alumina suspensions on density of green casts *Materials Research* 4, 4, (September 2001) (279-284), 1516-1439

Ilievski, D.; Austin, P. & Whittington, B. (2003). Studies into the internal structure of gibbsite agglomerates, *Chem. Eng. Technol.* 26, 3, (March 2003) (363-368), 0930-7516

Karimi-Lotfabad, S. & Gray, M. (2000). Characterization of contaminated soils using confocal laser scanning microscopy and cryogenic-scanning electron microscopy, *Environmental Science & Technology*, 34, 16, (August 2000) (3408-3414), 0013-936X

Kay, E.; Calloway, T.; Koopman, D.; Brigmon, R. & Eibling, R. (2003). Rheology Modifiers in Radioactive Waste Slurries, *Proceedings of ASME Fluid Eng. Div. Summer Meeting* pp. 855-863, 0-7918-3696-7 , Honolulu, Hawaii, USA, July 2003, ASME, New York

Kurtis, K.; El-Ashkar, N.; Collins, C. & Nalk, N. (2003). Examining cement-based materials by laser scanning confocal microscopy, *Cement & Concrete Composites*, 25, 7, (October 2003) (695-701), 0958-9465

Kurtis, K. & Monteiro, P. (2003). Chemical additives to control expansion of alkali-silica reaction gel: proposed mechanisms of control. *Journal of Materials Science*, 38, 9, (May 2003) (2027-2036), 0022-2461

Lau, C. & Dickinson, E. (2005). Instability and structural change in an aerated system containing egg albumen and invert sugar, *Food Hydrocolloids*, 19, 1, (January 2005) (111-121), 0268-005X

Liu, Q., Zhang, S., Sun, D. & Xu, J. (2009), Aqueous foams stabilized by hexylamine-Laponite particles, *Colloids and Surfaces A: Physicochem. Eng. Aspects*, 338, 1-3 (April 2009) (40-46), 0927-7577

Marusin, S. (1995). Sample preparation - The key to SEM studies of failed concrete. *Cement & Concrete Composites*, 17, 4, (1995) (311-318), 0958-9465

Mehta, P. & Monteiro, P. (2006). *Concrete - Microstructure, properties and materials*, McGraw-Hill, 0-07-146289-9, New York

Mohr, J. & Kurtis, E. (2006). Fractography of fiber-cement composites via laser scanning confocal microscopy, *Proceedings of 16th European conference on fracture, measuring, monitoring, and modeling concrete properties: in honor of Surendra P. Shah*, 503-508, Alexandroupolis, Greece

Pugh, J. (1994). Dispersion and stability of ceramic powders in liquids, *Surface and Colloid Chemistry in Advanced Ceramics Processing*, Marcel Dekker, New York, pg. 127-188

Ramachandran, V. (1998). Alkali-aggregate expansion inhibiting admixtures, *Cement & Concrete Composites*, 20, 2-3, (April-June 1998) (149-161), 0958-9465

Reed, M.; Howard, C. & Shelton, C. (1997). Confocal imaging and second-order stereological analysis of a liquid foam, *Journal of Microscopy*, 185, 3, (March 1997) (313-320), 0022-2720

Ribeiro, M.; Tulyaganov, D.; Ferreira, J. & Labrincha, J. (2004). Production of Al-rich sludge-containing ceramic bodies by different shaping techniques, *Journal of Materials Processing Technology*, 148, (May 2004) (139-146), 0924-0136

Ren, F.; Smith, I.; Baumann, M. & Case, E. (2005). Three-dimensional microstructural characterization of porous hydroxyapatite using confocal laser scanning microscopy, *Int. J Appl. Ceram. Technol.*, 2, 3, (2005) (200–211), 1546-542X

Russel, W. (1987). Theoretical approaches to the rheology of concentrated dispersions, *Powder Technology*, 51, (June 1987) (15-25), 0032-5910

Schmid, M.; Thill, A.; Purkhold, U.; Walcher, M.; Bottero, J.; Ginestet, P.; Nielsen, P., Wuertz, S. & Wagner, M. (2003). Characterization of activated sludge flocs by confocal laser scanning microscopy and image analysis, *Water Research*, 17, (May 2003) (2043-2052), 0043-1354

Selomulya, C.; Liao, J.; Bickert, G. & Amal, R. (2006). Micro-properties of coal aggregates: Implications on hyperbaric filtration performance for coal dewatering, *International Journal of Mineral Processing*, 80, 2-4, (September 2006) (189-197), 0301-7516

Spinelli, H. (1998). Polymeric Dispersants in Ink Jet Technology, *Adv. Mater.*, 10, 15, (October 1998) (1215-1218), 0935-9648

Tanaka, S.; Kato, Z.; Uchida, N. & Uematsu, K. (2003). Direct observation of aggregates and agglomerates in alumina granules, *Powder Technology*, 129, 1-3, (January 2003) (153-155), 0032-5910

Thill, A.; Wagner, M. & Bottero, J. (1999). Confocal scanning laser microscopy as a tool for the determination of 3D floc structure, *Journal of Colloid and Interface Science*, 220, 2, (December 1999) (465-467), 0021-9797

Vijayaraghavan, K.; Nikolov, A.; Wasan, D.; Calloway, B.; Crowder, M.; Stone, M. & Quershi, Z. (2006). Radioactive Waste Foams: Formation and Mitigation, *Journal of Environmental Engineering*, 132, 7, (July 2006) (716-724), 0733-9372

Wasan, T., Nikolov, D.; Shah, A., (2004), Foaming-antifoaming in boiling suspensions, *Ind. Eng. Chem. Res.*, 43, 14, (2004) (3812-3816), 0888-5885

White, T.; Stone, M.; Calloway, T.; Brigmon, R.; Eibling, R.; Nikolov, A.; Wasan, D. (2008). Understanding the effects of dispersant addition to slurry rheology using laser scanning confocal microscopy, *Separation Science and Technology*, 43, 9, (July 2008) (2859-2871), 0149-6395

Zamecnik, R., White, L.; Jones, M.; Hassan, M.; Eibling, E.; Duignan, R.; Crawford, L.; Calloway, B. (2003). Radioactive Waste Evaporation: Current Methodologies Employed for the Development, Design and Operation of Waste Evaporators at the Savannah River Site and Hanford Waste Treatment Plant, *Proceedings of ASME 2003 9th International Conference on Radioactive Waste Management and Environmental Remediation*, pp. 157-170, 0-7918-3732-7, Oxford, England, September 2003, ASME, New York

Zhang, S., Lan, Q., Liu, Q., Xu, J., Sun, D., (2008), Aqueous foams stabilized by Laponite and CTAB, *Colloids Surf.*, 317, 1-3, (March 2008) (406-413), 0927-7757


**Laser Scanning, Theory and Applications**
Edited by Prof. Chau-Chang Wang

ISBN 978-953-307-205-0
Hard cover, 566 pages
**Publisher** InTech
**Published online** 26, April, 2011
**Published in print edition** April, 2011

Ever since the invention of laser by Schawlow and Townes in 1958, various innovative ideas of laser-based applications emerge very year. At the same time, scientists and engineers keep on improving laser's power density, size, and cost which patch up the gap between theories and implementations. More importantly, our everyday life is changed and influenced by lasers even though we may not be fully aware of its existence. For example, it is there in cross-continent phone calls, price tag scanning in supermarkets, pointers in the classrooms, printers in the offices, accurate metal cutting in machine shops, etc. In this volume, we focus the recent developments related to laser scanning, a very powerful technique used in features detection and measurement. We invited researchers who do fundamental works in laser scanning theories or apply the principles of laser scanning to tackle problems encountered in medicine, geodesic survey, biology and archaeology. Twenty-eight chapters contributed by authors around the world to constitute this comprehensive book.



INTECH
open science | open minds

**InTech Europe**
University Campus STeP Ri
Slavka Krautzeka 83/A
51000 Rijeka, Croatia
Phone: +385 (51) 770 447
Fax: +385 (51) 686 166
www.intechopen.com

**InTech China**
Unit 405, Office Block, Hotel Equatorial Shanghai
No.65, Yan An Road (West), Shanghai, 200040, China
中国上海市延安西路65号上海国际贵都大饭店办公楼405单元
Phone: +86-21-62489820
Fax: +86-21-62489821

IntechOpen